Substituted Position Effect on Twisted Intramolecular Charge Transfer of 1- and 2-Anthracene Aromatic Carboxamides as Chemosensors Based on Linear Polyether

Jeongsik KIM,* Tatsuya MOROZUMI,** Hisafumi HIRAGA,** and Hiroshi NAKAMURA**†

**Division of Environmental Materials Science, Graduate School of Environmental Science,
 Hokkaido University, Sapporo, Hokkaido 060–0810, Japan*
***Section of Materials Science, Research Faculty of Environmental Earth Science, Hokkaido University,
 Sapporo, Hokkaido 060–0810, Japan*

Bi-chromophoric compounds linked to linear polyether *N,N′*-[oxybis(3-oxapentamethyleneoxy-2-phenyl)]-bis(1-anthracenecarboxamide) ($\mathbf{1_4}$) and its analogues ($\mathbf{1_5}$, $\mathbf{2_4}$ and $\mathbf{2_5}$) were synthesized. Their photochemical properties and complexation actions were investigated in acetonitrile. These fluoroionophores have shown weak emissions in the absence of guest ions, resulting in a twisted intramolecular charge transfer (TICT) quenching process (off state) of an anthracene aromatic amide moiety. After the formation of a complex with alkaline earth metal ions, a large enhancement of fluorescent intensities was obtained (on state). The efficiencies of controlling an off-on fluorescent signal using $\mathbf{1_4}$ and its analogues ($\mathbf{1_5}$, $\mathbf{2_4}$ and $\mathbf{2_5}$) were larger than that of the 9-positioned analogue. These results suggested that the TICT relaxation process was effectively able to control using $\mathbf{1_4}$ and its analogues ($\mathbf{1_5}$, $\mathbf{2_4}$ and $\mathbf{2_5}$) by complex formations.

Introduction

Complexations of metal ions with organic molecules are subjects of considerable interest as chemical sensors in various fields: biology, medicine, and environmental sciences.[1] Many kinds of crown ethers,[2-5] cyclodextrins[6] and calix[*n*]arenes[7,8] have been designed for the spectrophotometric determination of metal ions. In 1977, Takagi *et al.*[9] revealed an initial example of chromogenic crown ethers. These molecules, comprising a chromophoric moiety and a complexing part, can convert information produced by a metal binding event into an optical signal, such as color changes. Since their initial development, various chromogenic[10,11] and fluorometric[12] crown ethers have been developed. Chromogenic proton-dissociable lariat ethers, in which an acidic function is a part of a pendant chromophore unit, have attracted noticeable attention as prospective photometric reagents for metal-ion determination.[13,14] For such ligands, selective metal-ion recognition by a crown ether framework is coupled with a color change upon proton dissociation of the chromophore group. Monoprotic chromoionophores with a picrylamine moiety in the sidearm have been studied by Takagi *et al.*[9,15-18] and Pacey *et al.*[19-22] as colorimetric reagents for the selective recognition of alkali metal ions in solvent extraction systems.

The photochemical behaviors of chromoionophores with anthracene derivatives have been investigated as bichromophoric compounds in dimerization, energy transfer, charge transfer, *etc.*[23] Kakizawa *et al.* reported several fluorescent reagents that have two fluorescent chromophores (9-substituted anthracene) at both terminals of 1,13-diamino-4,7,10-trioxatridecane, and their complexation behaviors with alkali and alkaline earth cations were investigated.[24] This 9-anthracenecarboxamide derivative showed changes of fluorescence spectra from a monomer (400 nm) to an excimer (490 nm) through complexation with metal cations. On the other hand, 1- or 2-anthracenecarboxamide derivatives at both terminals of 1,13-diamino-4,7,10-trioxatridecane[25] yielded photodimerization in the presence of alkaline earth metal ions. Anthracene aliphatic amide derivatives showed alternative photochemical features, which have an excimer or photodimer according to the substitution position (9-substitution *vs.* 1- or 2-substitution).

Photophysical properties of the anthryl aromatic amide derivatives with the hope of widening this field of the study have been examined in our laboratory.[26-34] We also found that the fluorescence emissions of the *N*-phenyl-9-anthracenecarbox-
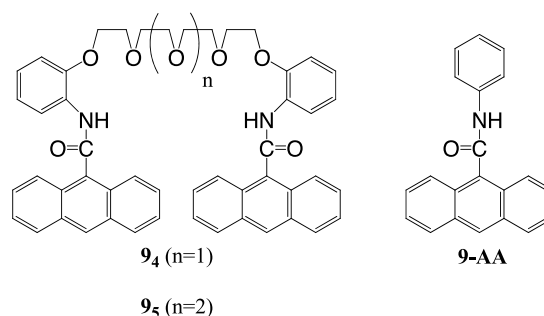

Fig. 1   Structures of $\mathbf{9_4}$, $\mathbf{9_5}$ and **9-AA**.

---

† To whom correspondence should be addressed.
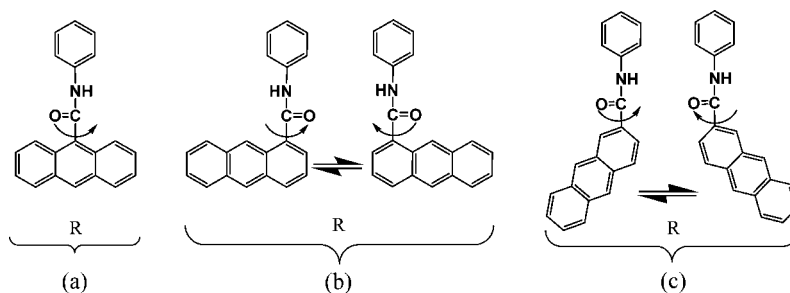E-mail: nakamura@ees.hokudai.ac.jp

Fig. 2   Schematic representation of the proposed rotation radii (R) of model compounds **9-AA** (a), **1-AA** (b), and **2-AA** (c).
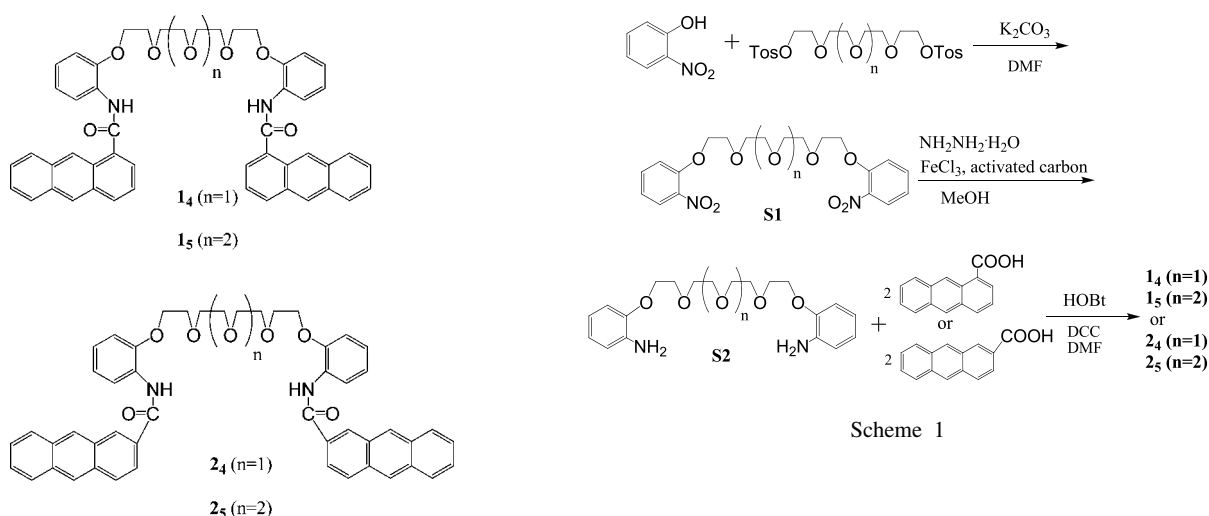

Fig. 3   Structures of 1_4, 1_5, 2_4 and 2_5.

amide unit (**9-AA**) and its derivatives (**9_4** and **9_5**) (Fig. 1) were almost quenched in solution.[30] This observation established that **9-AA** derivatives (**9_4** and **9_5**) show an intramolecular motion-assisted quenching of fluorescence (fluorescent: "off" state), such as a twisted intramolecular (internal) charge transfer (TICT) in the solvent. Upon the formation of a complex, loose helical structures of **9_4** and **9_5** were fixed by strong cooperative binding between the carbonyl and ethylenoxy moieties for metal ions. Therefore, the TICT relaxation pathway could be controlled by complexation; fluorescence emission of the **9-AA** moiety was observed (fluorescent: "on" state).

To obtain more effective "off-on" fluorescent signal changes, substituted position effects could be employed. Figure 2 shows three anthracene aromatic amides derivatives and all rotation of the anthracene rings around Ph–NH–CO– bond axis in the ground and excited states. It is clear that the sweeping areas and volumes by the rotation of anthracene rings in **1-** and **2-AA** are larger than those of **9-AA**. This increase of the sweeping area and the volume will induce an increase of the probability of receiving more effective steric repulsion at a binding event. This increase of steric repulsion will yield a desirable effect for controlling the TICT of **1-** and **2-AA**. With these ideas in mind, we synthesized new fluoroionophores 1_4, 1_5, 2_4 and 2_5 (Fig. 3), and investigated their complexation behaviors with alkaline earth cations.

Experimental

Synthetic method of the reagents 1_4, 1_5, 2_4, and 2_5

2-Nitrophenol (0.56 g, 0.04 mol) and K_2CO_3 (0.55 g, 0.04 mol) were dissolved in DMF (50 mL) and tetra- and pentaethylene glycol ditosylate (1.01 g and 1.09 g, respectively 0.02 mol) was added. The reaction solution was heated at 80°C for 3 days. The mixture was evaporated, and the residue was dissolved in toluene (50 mL). The toluene layer was washed in a 20% Na_2CO_3 aqueous solution several times. The toluene layer was evaporated to obtain compound **S1** (Scheme 1), which was used without further purification (yield: 58%). Compound **S1** (9.95 g, 0.022 mol), a small amount of $FeCl_3$ and 9 g of activated carbon were added to 80 mL of MeOH. The mixture was refluxed for 30 min. Then, $NH_2NH_2 \cdot H_2O$ (2.3 g, 0.044 mol) was carefully added into the solution. The mixture solution was refluxed for 4 h. The activated carbon was filtered off, and the methanol solution was evaporated. The residue was dissolved in 50 mL of $CHCl_3$. The organic layer was washed by a 20% Na_2CO_3 aqueous solution several times and evaporated to obtain compound **S2**. Compound **S2** (9.93 g, 0.02 mol) and HOBt (5.6 g, 0.04 mol) was dissolved in 50 mL of DMF, and each 0.04 mol of 1-anthracenecarboxylic acid or 2-anthracenecarboxylic acid was added. The solution was treated with dicyclohexylcarbodiimide (8.2 g, 0.04 mol) under stirring for 1 day at 0°C. The solvent was evaporated under reduced pressure, and a crude compound was obtained. Compounds 1_4, 1_5, 2_4, and 2_5 were purified by silica-gel column chromatography (Wakogel C-200, eluent; chloroform for 1_4; chloroform/hexane for 1_5; chloroform for 2_4; chloroform/ethyl acetate for 2_5) (Scheme 1). Their structures and purities were confirmed by ^{1}H NMR spectra and elemental analyses.
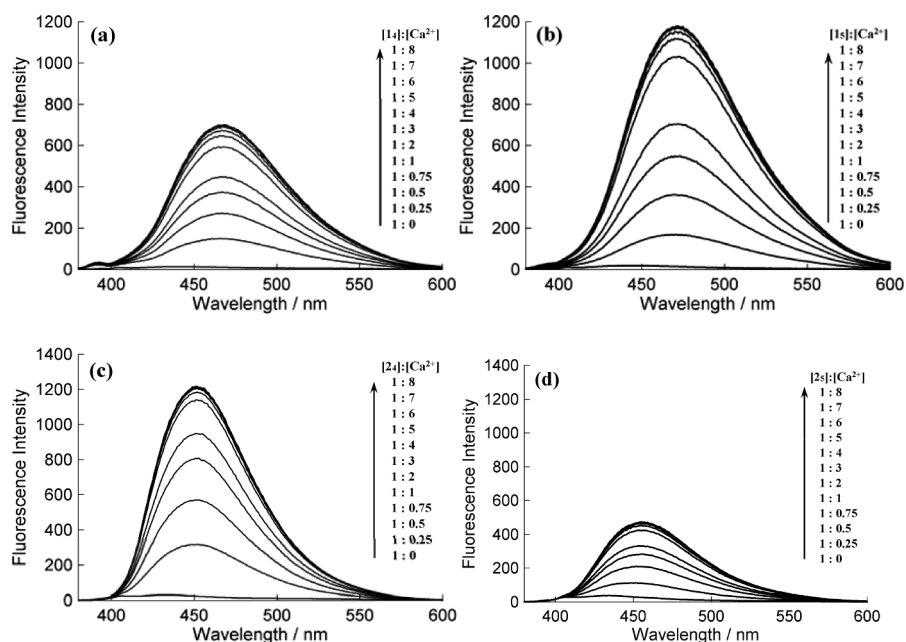
Scheme 1

Fig. 4   Fluorescence spectra of 1_4 (a), 1_5 (b), 2_4 (c), and 2_5 (d) and their Ca^{2+} complex in acetonitrile at 25°C. Excitation wavelength: 363 nm. [**L**] = 1 × 10^{-5} mol/dm^3. [Ca^{2+}]/[**L**] = 0, 0.25, 0.5, 0.75, 1, 2, 3, 4, 5, 6, 7, 8.

N,N′-(Oxybis(3-oxapentamethyleneoxy-2-phenyl))-bis(1-anthracenecarboxamide) (1_4)

   Yield 76.2%, m.p. 135 – 137°C. ^{1}H-NMR (acetonitrile-d_3) δ = 2.73 (–C–CH$_2$–O, t, 4H), 3.01 (–C–CH$_2$–O, t, 4H), 3.46 (–C–CH$_2$–O, t, 4H), 4.00 (–C–CH$_2$–O, t, 4H), 6.99 (aromatic, d, 2H), 7.11 (aromatic, m, 4H), 7.45 – 7.50 (aromatic, m, 6H), 7.73 (aromatic, d, 2H), 7.99 (aromatic, d, 2H), 8.03 (aromatic, d, 2H), 8.45 (aromatic, d, 4H), 8.69 (NH, s, 2H), 8.94 (aromatic, s, 2H). Found: C, 74.60; H, 5.56; N, 3.51%. Calcd. for C$_{50}$H$_{44}$O$_7$N$_2$·H$_2$O: C, 74.80; H, 5.67; N, 3.49%.

N,N′-(Ethylenedioxybis(3-oxapentamethyleneoxy-2-phenyl))-bis(1-anthracenecarboxamide) (1_5)

   Yield 73.3%, m.p. 140 – 142°C. ^{1}H-NMR (acetonitrile-d_3) δ = 2.85 (–C–CH$_2$–O, s, 2H), 2.90 (–C–CH$_2$–O, t, 4H), 3.16 (–C–CH$_2$–O, t, 4H), 3.56 (–C–CH$_2$–O, t, 4H), 4.07 (–C–CH$_2$–O, t, 4H), 7.03 – 7.11 (aromatic, m, 6H), 7.43 – 7.48 (aromatic, m, 6H), 7.55 (aromatic, d, 2H), 8.00 (aromatic, d, 4H), 8.10 (aromatic, d, 2H), 8.45 (aromatic, d, 2H), 8.49 (aromatic, s, 2H), 8.73 (NH, s, 2H), 8.95 (aromatic, s, 2H). Found: C, 74.36; H, 5.83; N, 3.37%. Calcd. for C$_{52}$H$_{48}$O$_8$N$_2$·1/2H$_2$O: C, 74.53; H, 5.89; N, 3.34%.

N,N′-(Oxybis(3-oxapentamethyleneoxy-2-phenyl))-bis-(2-anthracenecarboxamide) (2_4)

   Yield 74.8%, m.p. 121 – 123°C. ^{1}H NMR (acetonitrile-d_3) δ = 3.24 (–C–CH$_2$–O, t, 4H), 3.41 (–C–CH$_2$–O, t, 4H), 3.66 (–C–CH$_2$–O, t, 4H), 4.05 (–C–CH$_2$–O, t, 4H), 6.93 – 7.05 (aromatic, m, 6H), 7.45(aromatic, t, 4H), 7.66 (aromatic, d, 2H), 7.93 – 7.99 (aromatic, m, 6H), 8.29 (aromatic, d, 2H), 8.37 (aromatic, s, 2H), 8.46 (aromatic, s, 2H), 8.50(aromatic, s, 2H), 8.87 (NH, s, 2H). Found: C, 76.16; H, 5.62; N, 3.59%. Calcd. for C$_{50}$H$_{44}$O$_7$N$_2$: C, 76.08; H, 5.68; N, 3.55%.

N,N′-(Ethylenedioxybis(3-oxapentamethyleneoxy-2-phenyl))-bis(2-anthracenecarboxamide) (2_5)

   Yield 71.5%, m.p. 88 – 90°C. ^{1}H NMR (acetonitrile-d_3) δ =
3.05 (–C–CH$_2$–O, s, 2H), 3.22 (–C–CH$_2$–O, t, 4H), 3.44 (–C–CH$_2$–O, t, 4H), 3.72 (–C–CH$_2$–O, t, 4H), 4.13 (–C–CH$_2$–O, t, 4H), 6.99 – 7.07 (aromatic, m, 6H), 7.46 (aromatic, m, 4H), 7.81 (aromatic, d, 2H), 7.79 – 8.03 (aromatic, m, 6H), 8.35 (aromatic, d, 2H), 8.42 (aromatic, s, 2H), 8.52 (aromatic, d, 4H), 8.93 (NH, s, 2H). Found: C, 73.71; H, 5.93; N, 3.28%. Calcd. for C$_{52}$H$_{48}$O$_8$N$_2$·H$_2$O: C, 73.74; H, 5.95; N, 3.31%.

Measurement of fluorescence and UV spectra

   Fluorescence spectra were measured using a Shimadzu RF-5300PC at 25°C. UV spectra were recorded on a Shimadzu UV-2400 at 25°C. The concentrations of the fluorescent reagents were 1 × 10^{-5} mol/dm^3 in purified acetonitrile. Alkaline-earth-metal cations were added to a solution of the fluorescent reagent as perchlorate salts. The temperature for all measurements was maintained at 25°C. The excitation wavelength was 363 nm.

Measurement of ^{1}H NMR

   ^{1}H NMR spectra were measured using a JEOL JNM-EX400 at 30°C. In the case of measurements of the metal complexes, excess amounts of metal cations as perchlorate salts were added to these solutions.

Results and Discussion

Fluorescence response ratio (I_{max}/I_0) and complex formation constants

   Figure 4 shows fluorescence spectra of 1_4 (a), 1_5 (b), 2_4 (c), and 2_5 (d) in the absence and presence of Ca^{2+}. Table 1 also lists the fluorescence maxima (λ_{max}), the fluorescence response ratio (I_{max}/I_0), and complex formation constants (log K) of metal complexes of 1_4 – 2_5 in acetonitrile at 25°C. The experimental data of 9_4 and 9_5 are sited in Table 1 as a comparison from Ref. 30. Fluorescence emissions of the anthracene moiety in 1_4 – 2_5 were faint in the absence of metal ions as shown in

Table 1   Fluorescence maxima (λ_{max}), fluorescent response ratio (I_{max}/I_0) at λ_{max} and complex formation constants (log K)[a] of metal complexes in acetonitrile at 25°C

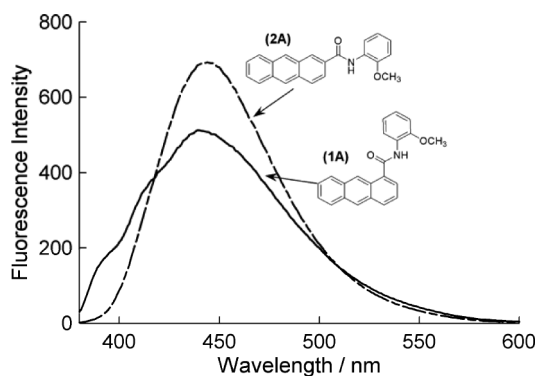| Ligand	Guest ion	λ_{max}/nm	I_{max}/I_0	log K
1_4	Ca^{2+}	467	62.9	5.77
	Sr^{2+}	459	39.2	5.23
	Ba^{2+}	458	22.5	4.55
1_5	Ca^{2+}	471	73.9	6.72
	Sr^{2+}	460	52.6	5.64
	Ba^{2+}	456	45.1	5.24
2_4	Ca^{2+}	452	50.2	6.08
	Sr^{2+}	447	37.1	5.42
	Ba^{2+}	445	19.6	5.03
2_5	Ca^{2+}	456	16.8	6.42
	Sr^{2+}	449	15.6	5.61
	Ba^{2+}	445	17.2	5.45
9_4	Ca^{2+}	445	22.7	5.67
	Sr^{2+}	445	18.6	4.35
	Ba^{2+}	445	13.6	4.53
9_5	Ca^{2+}	445	38.5	6.57
	Sr^{2+}	445	34.2	5.71
	Ba^{2+}	445	33.2	5.81

a. $K = [1 \cdot M^{2+}]/[1][M^{2+}]$.

Fig. 5   Fluorescence spectra of model compounds, *N*-(2-methoxyphenyl)-1-anthracenecarboxamide (solid line) and *N*-(2-methoxyphenyl)-2-anthracenecarboxamide (dotted line). [**1A**] = 1.3×10^{-5} mol/dm³ and [**2A**] = 1.6×10^{-5} mol/dm³ in glycerin (containing 1% (vol.) DMF).

Fig. 4.   On the other hand, structureless broad spectra having a fluorescence emission maximum (λ_{max}) at around 452 – 471 nm (Table 1) was observed for all compounds.   The fluorescence intensities increased with the addition of Ca^{2+}, Sr^{2+}, and Ba^{2+}.   The increase of fluorescence emissions clearly depended on the metal-ion concentration; the spectra with maximum intensities are expected to be those of their complexes.   The fluorescent response values (I_{max}/I_0) for Ca^{2+} in 1_4, 1_5 and 2_4 were larger than those for Sr^{2+} and Ba^{2+}.   Notably, the value (73.9) for $1_5 \cdot Ca^{2+}$ was the largest in these series.   The order of I_{max}/I_0 for 1_4, 1_5 and 2_4 was $Ca^{2+} > Sr^{2+} > Ba^{2+}$.   Especially, 1_4 and 1_5 gave larger I_{max}/I_0 values than those of 2_4, 2_5, 9_4 and 9_5 for each metal cation.   This result suggests that 1-position is suitable for controlling TICT upon complexation.   On the other hand, 2_5 exhibited almost the same I_{max}/I_0 values for these metal cations.

To confirm the chemical species that gave these fluorescence emissions upon complexaton, a model study was carried out using *N*-(2-methoxyphenyl)-1-anthracenecarboxamide (**1A**) and 2-anthracene analogue (**2A**).   Figure 5 shows fluorescence
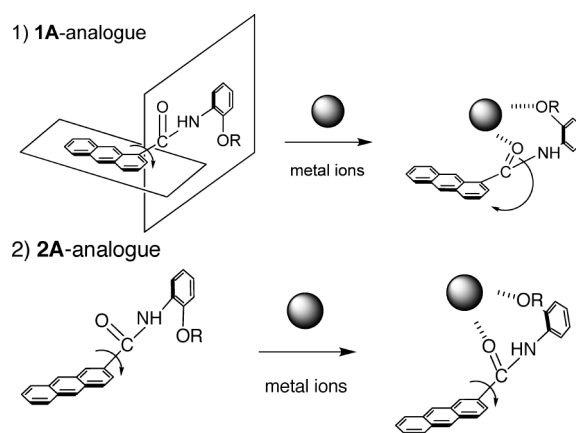

Fig. 6   Schematic representation of the molecular configuration of **1A**-analogue (1_4 and 1_5) and **2A**-analogue (2_4 and 2_5) before and after the addition of metal cations.   Oxyethylene and terminal benzene moieties in the ligand were omitted for clarity.

spectra of **1A** and **2A** in glycerin.   Since molecular motions should be slow in viscous media, such as glycerin, the twisted motion is frozen, resulting in large fluorescent emission.   The fluorescence emission of **1A** and **2A** gave a structureless broad peak, which is attributed to exciplex emission by a charge-transfer interaction between an anthracene ring and an amide moiety, while *N*-(2-methoxyphenyl)-9-anthracenecarboxamide shows a structured anthracene-like peak with λ_{max} of 415 nm in glycerin.[30]   The fluorescence maximum (λ_{max}) of **2A** was observed at 448 nm, which has a similar value to those of 2_4 and 2_5 complexes.   On the other hand, the fluorescence maximum (λ_{max}) of **1A** was obtained at 440 nm.   This value was different from λ_{max} of the 1_4 and $1_5 \cdot Ca^{2+}$ complexes (467 nm for 1_4 and 471 nm for 1_5).   This phenomenon will be ascribed to a position of the methoxy group and the carbonyl group and a π-interaction between the carbonyl group and the anthracene ring.   Figure 6 depicts a schematic representation of the molecular configuration of the **1A**-analogue (1_4 and 1_5) and **2A**-analogue (2_4 and 2_5) before and after the addition of metal cations.   The carbonyl group of the **1A**-analogue lies at an opposite (*trans*) position against the methoxy group so as to avoid a steric repulsion, corresponding to short wavelength, as shown in Fig. 5.   The carbonyl group also remained in a nearly perpendicular geometry against the anthracene ring to avoid a steric crowd from the 9-proton and the 2-proton (Fig. 6).   Meanwhile, in case of 1_4 and 1_5 metal-ion complexes, the carbonyl group had to be turned in the same direction (*cis*) to the methoxy group by the binding metal ion.   This geometry change induces a charge-transfer interaction between the carbonyl group and the anthracene ring upon complexation.   Therefore, ligands 1_4 or 1_5 upon complexation showed longer wavelength emission than that before binding with metal ions.   In the case of **2A**, 2_4 and 2_5, since the 2-position had a margin for a steric jam around the amide moiety and its 1- and 3-proton, both of the **2A** and 2_4, 2_5 complexes showed similar fluorescence spectra.   The **2A**-analogue (2_4 and 2_5) indicated no significant π-interaction changes between the anthracene ring and the amide moiety before and after complexation with all metal ions (Table 1).

The fluorescence emission intensity was increased by the addition of metal ions (Fig. 4).   The degree of the increase clearly depends on the concentrations of alkaline earth metal ions, and reflects the formation of the complex.   The formation

Table 2   Chemical shifts (δ, ppm) of 1_4 – 2_5 and their changes upon complexation with various cations[a]

		a	b	c	d	e	f	g	h	i	j	k	l	m	n	o	p	q	r	s
1_4	Free		2.73	3.01	3.46	4.00	7.01	7.12	7.10	8.48	8.70	8.00	7.43	8.07	8.44	8.00	7.49	7.49	7.73	8.94
	Ca²⁺		0.13	0.29	0.40	0.30	−0.06	−0.01	−0.08	−1.30	0.63	−0.15	0.10	0.13	0.15	−0.01	−0.01	−0.01	0.29	−0.16
	Sr²⁺		0.06	0.30	0.38	0.30	0.15	0.04	−0.04	−1.27	0.44	−0.23	0.06	0.13	0.15	0.04	0.04	0.04	0.18	−0.09
	Ba²⁺		0.07	0.21	0.24	0.15	0.07	0.08	−0.02	−1.00	0.21	−0.34	0.00	0.06	0.07	−0.03	−0.13	−0.13	0.03	−0.23
1_5	Free	2.86	2.90	3.16	3.57	4.08	7.05	7.11	7.07	8.45	8.73	7.75	7.48	8.11	8.49	8.00	7.47	7.47	8.01	8.94
	Ca²⁺	0.05	0.24	0.52	0.17	−0.06	0.00	0.18	0.05	−0.79	0.52	0.08	0.08	0.11	0.10	0.04	0.03	0.03	−0.12	−0.20
	Sr²⁺	0.16	0.21	b	0.18	−0.04	−0.03	0.13	0.01	−0.80	0.30	0.04	0.03	0.05	0.05	0.01	0.00	0.00	−0.15	−0.19
	Ba²⁺	−0.21	0.07	0.35	0.31	0.11	−0.11	0.10	0.05	−0.94	0.28	0.03	0.01	0.06	0.06	0.02	−0.03	−0.03	−0.16	−0.18
2_4	Free		3.24	3.41	3.66	4.06	6.96	7.05	7.01	8.30	8.88	7.77	7.99	8.38	7.97	7.45	7.45	7.97	8.50	8.46
	Ca²⁺		0.43	0.48	b	0.30	−0.06	−0.09	−0.05	−1.28	0.55	0.19	0.22	0.20	0.10	0.11	0.11	0.14	0.23	0.32
	Sr²⁺		b	0.38	0.29	0.19	0.10	−0.03	0.01	−1.21	0.31	0.15	0.15	0.15	0.18	0.18	0.18	0.18	0.13	0.26
	Ba²⁺		0.39	0.38	0.31	0.27	0.31	0.08	0.23	−0.95	0.34	0.16	0.18	0.19	0.12	0.13	0.13	0.12	0.15	0.30
2_5	Free	3.06	3.23	3.45	3.72	4.13	7.02	7.06	7.02	8.36	8.94	7.81	8.02	8.42	7.98	7.47	7.47	7.98	8.52	8.52
	Ca²⁺	0.52	0.26	0.25	0.02	−0.15	−0.03	0.11	−0.06	−0.84	0.18	−0.13	−0.09	−0.10	−0.09	−0.07	−0.07	−0.09	−0.06	0.01
	Sr²⁺	b	b	b	0.05	−0.09	0.08	0.18	0.03	−0.79	0.09	0.03	0.04	0.04	0.04	0.04	0.04	0.04	0.06	0.13
	Ba²⁺	0.52	0.35	0.31	0.16	0.02	0.01	0.09	0.03	−0.89	0.10	0.02	0.00	0.00	0.00	0.01	0.01	0.00	0.01	0.09

a. Positive values show lower field shifts, and negative values show higher field shifts. The values in "Free" indicate the chemical shifts (δ, ppm, from TMS) of the protons in acetonitrile-d_3 at 30°C.   b. These values could not be assigned due to overlapping of the peak of water.

of complexation with metal ions will eventually inhibit the TICT quenching of these fluorophores. The complex formation constants (log K) were evaluated from these data using a nonlinear least-squares curve-fitting method (Marquardt's method).[35]   The formation constants for these ligands with various cations were determined, as presented in Table 1.

In all cases, Ca²⁺ complexes of 1_4 – 2_5 gave the largest complex formation constants (log K). These data suggest that the affinity of the tetra- and penta-ethyleneoxide moiety for Ca²⁺ was better than that for Sr²⁺ and Ba²⁺; this tendency was the same as that shown by our previous data.[30]   The order of log K was Ca²⁺ > Sr²⁺ > Ba²⁺ for all chemosensors.   The configuration of 9_5,[30] which is a helical conformer with a pseudocyclic cavity containing penta ethyleneoxide, gave larger log K values than 9_4 containing tetra ethyleneoxide, and the same tendency was also observed in these series, 1_4 – 2_5.   It is readily apparent that complexes with more ethyleneoxide units are more stable.

UV absorption spectra of compounds 1_4 – 2_5

Figure 7 depicts typical UV spectra of 1_4 (a), 2_4 (b) and their Ca²⁺ complexes. The arrow in the figure indicates the direction for the changed spectrum with increasing the concentration of the metal ion.   The UV absorption band of 1_4·Ca²⁺ (Fig. 7a) around 280 – 330 nm, which can be assigned to the benzene–NH–CO moieties, decreased concomitantly with the increased Ca²⁺ concentration.   Identical results were observed using 1_4 and 1_5 in the presence of Ca²⁺, Sr²⁺, and Ba²⁺.   The 1_4·Ca²⁺ complex at around 370 nm showed a broader structure than that of free 1_4, while 9_n showed almost no UV spectral changes at complexation.[30]

The UV spectra of free 2_4 (Fig. 7b) showed a structureless shape.   This phenomenon is expected to result from intramolecular charge transfer from benzene to anthracene units of the compound.   The UV spectra of 2_4 gradually changed to a structured shape with four peaks (around 340, 360, 375, and
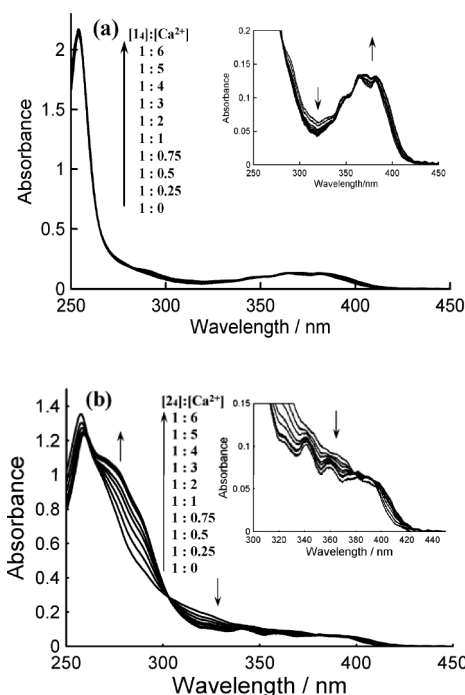
Fig. 7   UV spectra of 1_4 (a) and 2_4 (b) and their Ca²⁺ complex in acetonitrile at 25°C. [**L**] = 1 × 10⁻⁵ mol/dm³, [Ca²⁺]/[**L**] = 0, 0.25, 0.5, 0.75, 1, 2, 3, 4, 5, 6.

390 nm) with the addition of Ca²⁺.   That result demonstrates that the charge-transfer characteristics between the anthracene and amide group were reduced by complexation.
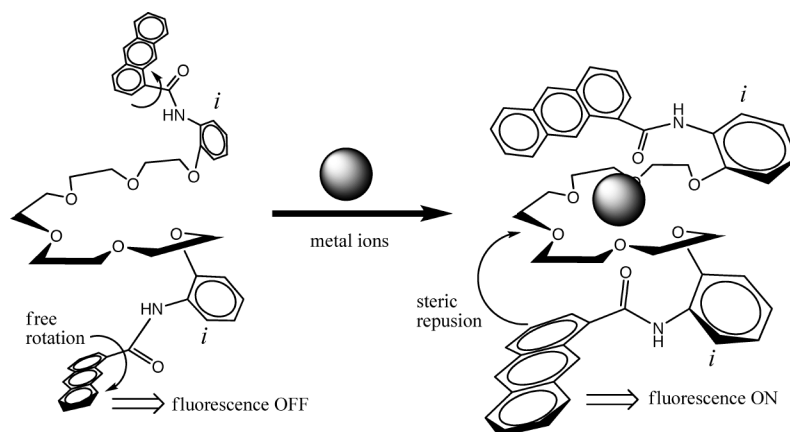
Fig. 8   Schematic representation of the proposed structural change of 1_5 before and after the addition of metal ions in the ground state.

¹H NMR measurements

To clarify the structures of the complexes, a ¹H NMR examination was performed in both the absence and presence of metal cations in acetonitrile-d_3 at 30°C. Peak assignments were made using H–H COSY and NOESY spectra. The chemical shift of 1_4 – 2_5 and their induced chemical shift changes upon the formation of complexes with various metal ions are presented in Table 2.

Unusually high field chemical shifts (*ca.* 2.7 – 2.9 ppm) for ethylene protons *a* and *b* of free 1_4 and 1_5 were obtained. Usually, this peak position of oxyethylene is observed at *ca.* 3.5 ppm.   The differences of these shifts are attributable to a diamagnetic ring current of aromatic groups.   The protons are positioned above the anthracene moieties; consequently, unusually high field chemical shifts are observed.   The same trends in ¹H NMR studies were also obtained in free 9_4 and 9_5.[30]

Proton *i* showed considerable chemical shift changes upon complexation. The same results were obtained in a previous study.[30]   Thus, the characteristic NMR behavior of aromatic *ortho* proton *i* in 1_4 – 2_5 can be explained as follows: the ethyleneoxy moiety was positioned in the anti direction of the carbonyl group (*trans* position) to avoid a steric repulsion. After coordination with alkaline earth metal ions, the carbonyl group turned toward the same direction of the ethyleneoxy moiety (*cis* position) by the coordinated metal ion.   In this configuration change, proton *i* goes out of the deshielding area of the carbonyl group; the anomalous chemical shift goes back to the normal value.

Considerable chemical shift changes of protons on the benzene ring (*f* – *h*) in 1_4 – 2_5 were not observed upon complexation with any metal ion.   This result indicated that almost no π–π interactions exist between the anthracene and the benzene ring.

In the 1_4·Ca²⁺ complex, oxyethylene proton peaks (protons *c*, *d*, *e*) shifted to a low magnetic field ($\Delta\delta$ = 0.29, 0.40, and 0.30 ppm, respectively) because of a reduction of the electron density on the oxygen atoms by the coordinated cations. Additionally, a large low magnetic field shift of amide proton *j* was observed ($\Delta\delta$ = 0.63 ppm).   On the other hand, proton *b* showed no marked chemical shift change.   These observations indicated that Ca²⁺ was mainly bound by the carbonyl group and the two oxygen atoms attached to protons *c* – *e*.   The latter observation suggests that proton *b* was placed in the deshielding zone of the anthracene ring.   Rotations of OC–N and N–benzene bonds were inhibited through a strong cooperative coordination by Ca²⁺

when the anthracene moiety of 1_4·Ca²⁺ was excited. Furthermore, the existence of proton *b* can provide an obstacle to rotation along the anthracene–CO bond.

The ethylene proton peaks *b* – *d* of the 1_5·Ca²⁺ complex shifted to a low magnetic field ($\Delta\delta$ = 0.24, 0.52, and 0.17 ppm, respectively) because of a reduction of the electron density of the oxygen atoms through complexation. A large low magnetic field shift of the amide proton *j* was observed ($\Delta\delta$ = 0.52 ppm). On the other hand, no remarkable chemical shift changes of protons *a* and *e* were observed. These results indicate that Ca²⁺ was mainly bound to the carbonyl group and oxygen atoms in the ethyleneoxy moiety. It is noteworthy that the chemical shift changes of proton *a* in 1_5·Ba²⁺ gave a high magnetic field shift ($\Delta\delta$ = –0.21 ppm). This result arises from the anthracene ring current which indicates that proton a and the protons of the anthracene ring are close together.

The protons on the oxyethylene units of 2_4 shifted to a low magnetic field in the presence of Ca²⁺, Sr²⁺, and Ba²⁺. Amide proton *j* exhibited considerably large low magnetic field shifts for metal cations. In contrast to 1_4 and 1_5, the anthracene rings and oxyethylene units of 2_4 are not close to each other upon complexation.

The ethylene proton *a* in 2_5 shifted to a lower magnetic field ($\Delta\delta$ = 0.52 ppm) in Ca²⁺ and Ba²⁺ complex than that of 1_5, which has the same ethylene chain length. Amide proton *j* exhibited no chemical shift change compared to other compounds.   The present ¹H NMR data show that the two oxygen atoms attached to carbons *a* and *b* of 2_5 bound strongly to metal ions, and proton *j* did not have a strong coordination. The chemical shift changes of the oxyethylene moiety and protons *i* and *j* showed almost no chemical shift changes according to ionic radii. This fact indicates that the structural property of 2_5 does not depend on the ionic size. In all cases, no protons of the anthracene ring showed significant chemical shift changes during complexation with any metal ion. These results underscore that no π–π interaction exists between the two anthracene rings.

Based on the fluorescence and ¹H NMR data, an expected complex structure of 1_5 is depicted in Fig. 8 as a typical result. The TICT relaxation process of the 1-anthryl moiety is better controllable by a steric repulsion with the polyether-chain following their large rotation radius upon complexation with metal cations (Fig. 7). These observations are consistent with the fact that the fluorescent response ratio (I_{max}/I_0) of the

1-anthryl substituents (1_4 and 1_5) was larger than that of the 9-anthryl substituents (9_4 and 9_5) having a small rotation radius and 2-anthryl substituents (2_4 and 2_5) taking a restricted rotation axis, which is not close to a polyether-chain.

Conclusions

We examined the absorption and fluorescence spectra of symmetric linear polyether derivatives (1_4 – 2_5) containing 1- and 2-anthracene aromatic amide. The spectral behaviors of the compounds were elucidated and compared to those of 9-anthracene aromatic amide derivatives. Compounds 1_4 - 2_5 exhibited TICT quenching through rotation around the anthracene–CO, OC–NH, and N–C (benzene) bonds at the excited state in an acetonitrile solution. The rotations of these three bonds in 1_4 – 2_5 were controlled by the formation of complexes with Ca^{2+}, Sr^{2+}, and Ba^{2+}. These alkaline earth cation complexes showed large enhancement effects on the fluorescence intensity as an "Off-On" fluorescence signal. The results of this study showed that stabilization of complex and the structural changes of the ligand depend on the chain length of the oxyethylene moiety and the position of anthracene substitution: better I_{max}/I_0 values were obtained for 1_4 and 1_5 than for 2_4 and 2_5. It can be concluded from these results that 1-substituted anthracene provides effective inhibition of the rotation of the anthracene–CO bond in the excited state.

References

 1. A. P. de Silva, H. Q. N. Gunaratne, T. Gunnlaugsson, A. J. M. Huxely, C. P. McCoy, J. T. Rademacher, and T. E. Rice, *Chem. Rev*., **1997**, *97*, 1515.
 2. S. Fery-Forgues, M. T. Le Bris, J. P. Guettt, and B. Valeur, *J. Chem. Soc., Chem. Commun*., **1988**, 384.
 3. J. Bourson and B. Valeur, *J. Phys. Chem*., **1989**, *93*, 3871.
 4. S. Fery-Forgues, J. Bourson, L. Dallery, and B. Valeur, *New J. Chem*., **1990**, *14*, 617.
 5. J. Bourson, M. N. Borrel, and B. Valeur, *Anal. Chim. Acta*, **1992**, *257*, 189.
 6. W. Saenger, *Angew. Chem., Int. Ed. Engl*., **1980**, *19*, 344.
 7. S. Shinkai, *Tetrahedron*, **1993**, *49*, 8933.
 8. K. Tsubaki, T. Morimoto, T. Otsubo, T. Kinoshita, and K. Fuji, *J. Org. Chem*., **2001**, *66*, 4083.
 9. M. Takagi, H. Nakamura, and K. Ueno, *Anal. Lett*., **1977**, *10*, 1115.
10. P. D. Beer, Z. Chen, P. A. Gale, J. A. Heath, R. J. Knubley, M. I. Ogden, and M. G. B. Drew, *J. Inclusion Phenom. Mol. Recognit. Chem*., **1994**, *19*, 343.
11. P. D. Beer, Z. Chen, and P. A. Gale, *Tetrahedron*, **1994**, *50*, 931.
12. J. A. A. W. Elemans, R. Hameren, R. J. M. van Nolte, and A. E. Rowan, *Adv. Mater*., **2006**, *18*, 1251.
13. G. W. Gokel, W. M. Leevy, and M. E. Weber, *Chem. Rev*., **2004**, *104*, 2723.
14. H. Nakamura, H. Sakka, M. Takagi, and K. Ueno, *Chem. Lett*., **1981**, 1305.
15. R. A. Bartsch, H. S. Hwang, V. S. Talanov, G. G. Talanova, and D. W. Purkiss, *J. Org. Chem*., **1999**, *64*, 5341.
16. H. Nakamura, M. Takagi, and K. Ueno, *Talanta*, **1979**, *26*, 921.
17. H. Nakamura, M. Takagi, and K. Ueno, *Anal. Chem*., **1980**, *52*, 1668.
18. Y. Katayama, R. Fukuda, and M. Takagi, *Anal. Chim. Acta*, **1986**, *185*, 295.
19. G. E. Pacey and B. P. Bubnis, *Anal. Lett*., **1980**, *13*, 1085.
20. G. E. Pacey, Y. P. Wu, and B. P. Bubnis, *Analyst*, **1981**, *106*, 636.
21. B. P. Bubnis and G. E. Pacey, *Talanta*, **1984**, *31*, 1149.
22. B. P. Bubnis, J. L. Steger, Y. P. Wu, L. A. Meyers, and G. E. Pacey, *Anal. Chim. Acta*, **1982**, *139*, 307.
23. H. D. Becker, *Chem. Rev*., **1993**, *93*, 145.
24. Y. Kakizawa, T. Akita, and H. Nakamura, *Chem. Lett*., **1993**, 1671.
25. H. Hiraga, T. Morozumi, and H. Nakamura, *Eur. J. Org. Chem*., **2004**, 4680.
26. Y. Suzuki, T. Morozumi, Y. Kakizawa, R. A. Bartsch, T. Hayashita, and H. Nakamura, *Chem. Lett*., **1996**, 617.
27. R. Tahara, T. Morozumi, Y. Suzuki, Y. Kakizawa, T. Akita, and H. Nakamura, *J. Inclusion Phenom*., **1998**, *32*, 283.
28. Y. Suzuki, T. Morozumi, H. Nakamura, M. Shimomura, T. Hayashita, and R. A. Bartsch, *J. Phys. Chem. B*, **1998**, *102*, 7910.
29. T. Anada, T. Kitaoka, H. Ota, Y. Kakizawa, Y. Akita, T. Morozumi, and H. Nakamura, *Bunseki Kagaku*, **1999**, *48*, 1107.
30. T. Morozumi, T. Anada, and H. Nakamura, *J. Phys. Chem. B*, **2001**, *105*, 2923.
31. T. Morozumi, H. Hiraga, and H. Nakamura, *Chem. Lett*., **2003**, *32*, 146.
32. J. Kim, T. Morozumi, and H. Nakamura, *Org. Lett*., **2007**, *9*, 4419.
33. J. Kim, T. Morozumi, N. Kurumatani, and H. Nakamura, *Tetrahedron. Lett*., **2008**, *49*, 1984.
34. J. Kim, T. Morozumi, and H. Nakamura, *Tetrahedron*, **2008**, *64*, 10735.
35. D. W. Marquardt, *J. Soc. Ind. Appl. Math*., **1963**, *11*, 431.